

# Optical properties of films of II-VI ternary semiconductor compounds deposited by chemical method

A. OUDHIA\*, R. DEWANGAN, P. C. CHOUBEY

*Department of Physics, Government V. Y.T. Autonomous PG College, Durg (Chhattisgarh), India*

*Affiliated to: Pt. Ravishankar Shukla University, Raipur, (Chhattisgarh), India*

The present paper consists of some interesting results of optical absorption and reflectance spectral studies of some chemically deposited films of CdS-Se relevant for applications in opto- electronics. The parameters like band gap, Urbach energy, extinction coefficient and refractive index are calculated using the data obtained by different studies. Moreover it describes a simple and cost effective method to obtain belt like morphology with approximate thickness between 125nm – 166nm, found to be advantageous for many practical applications.

(Received August 14, 2012; accepted March 13, 2014)

**Keywords:** Urbach energy, Deposition from liquid phase, II–VI compounds, Spectral reflectance, Optical absorption

## 1. Introduction

The CdS, CdSe and CdS–Se semiconductors have potential application in the field of light emitting diodes, laser diodes, photodiodes, optoelectronic switches, optical filters etc. [1]. These materials produce lasing in the visible spectral region. The defect reactions in these materials result in some characteristic changes in electrical, photoelectric and optical properties [2]. Because of the high photosensitivity of these materials are being utilized in photo resistors, optical filters, signal memory devices, laser screens, optoelectronic switches, electro-photography, image intensifiers and exposure meters [3]. So the structural characterization and spectral studies are certainly important for understanding afore mentioned newer applications of such materials. The present paper consists of a simple CBD method of deposition of CdS-Se nano belts along with some interesting results of their SEM, XRD, optical absorption, and reflectance spectral studies. Some important optical parameters are also calculated based on these studies.

## 2. Experimental

Films were prepared on glass substrates in a water bath by mixing appropriate amount of 1M solutions of cadmium acetate, thiourea, triethanolamine, and .01M solution of CdCl<sub>2</sub> prepared in double distilled water. 30% aqueous ammonia was added till the pH of the chemical bath became ~ 11. The source of selenide ions was a freshly prepared solution of sodium seleno sulphate. The cleaned glass slides were dipped vertically in the chemical bath at 60° C for one hr. The deposition was based on precipitation followed by condensation. Films were deposited in static condition. For the study of optical absorption and reflectance spectra Shimadzu (UV–VIS)

Pharmaspec-1700 spectrophotometer was used. XRD and SEM studies were performed at IUC-DAE Indore, using models Rigaku RU: H2R horizontal Rota flex and JEOL-JSM 5600 respectively.

## 3. Result and discussion

3.1: Extinction coefficient  $k$  is calculated using the following formula

$$k = \alpha\lambda/4\pi t$$

Where  $t$ , is the thickness of the film and  $\lambda$  is the wavelength of the source used, both measured in nm units [4].

3.2: Thickness measurement was done by a simple interference method. For this the film deposited on the substrate is again coated with a heavy and highly reflecting metal like aluminium to form a sharp step on the film edge. Another glass slide coated partially with the same metal, known as reference plate is then placed over the specimen with their metal –coated surface in contact with each other such that a small air gap is created at the step. A monochromatic parallel beam of light passing through a beam splitter or a glass plate inclined at 45° is then incident on the two–plate assembly and reflected light is then observed through the microscope. Sharp interference fringes (Fizeau) due to multiple reflections perpendicular to the step with equal displacements is observed [5]. The thickness can be determined using the relation –

$$t = b\lambda/ 2a$$

Where, 'b' is the displacement of the fringes at the step and 'a' is the distance between consecutive fringes. This technique is capable of resolution as low as 20 – 30 Å.

In present study the thicknesses of the films increased with the increase in the selenium content. The thickness of CdS film was measured to be 0.1711µm, and that of CdS<sub>0.95</sub>Se<sub>0.05</sub> and CdS<sub>0.70</sub>Se<sub>0.30</sub> was 0.2622 µm and 0.4149 µm respectively.

3.3: The Urbach energy is defined through the exponential dependence of the optical absorption on energy expressed as:

$$\alpha = \alpha_0 (\exp [(h\nu - h\nu_0) / \Delta])$$

$$\log \alpha = [(h\nu - h\nu_0) / \Delta] + \log \alpha_0$$

Where  $\Delta = kT / \alpha$ , is defined as the Urbach energy, obtained by the inverse slope of the graph between  $\log \alpha$  vs.  $h\nu$ . The unit of Urbach energy being eV [6].

3.4: The refractive index n of the films was calculated from the reflectance spectra using the formula given below [7-8]

$$n = n_s [(1 + R^{1/2}) / (1 - R^{1/2})]$$

where  $n_s$  is the refractive index of the substrate, 1.5 for glass in present case, and R is the reflectance at different wavelengths.

3.5 The grain size was calculated using the Scherrer Formulae [9,10]

$$D = 0.94\lambda / \beta \cos\theta.$$

The Dislocation Densities were calculated using the formula [11]:

$$\delta = 1/(D)^2.$$

## 4. Structural studies

### 4.1 SEM studies

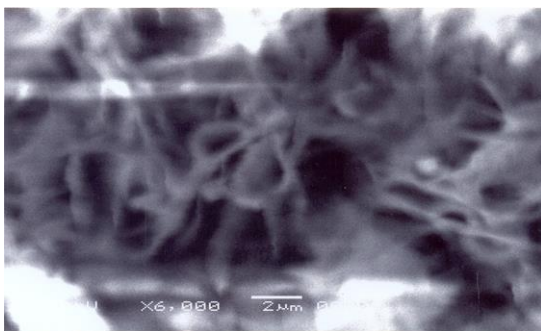


Fig. 1a. SEM of CdS<sub>0.95</sub>Se<sub>0.05</sub> film.

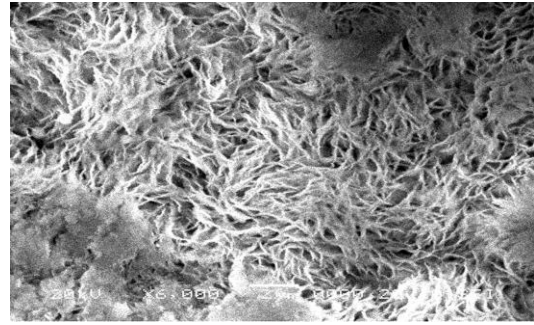


Fig. 1b. SEM of CdS<sub>0.70</sub>Se<sub>0.30</sub> film.

The SEM micrographs of the films with two different concentrations of CdSe are shown in Fig. 1a and 1b respectively. Both figures consist of leafy structures showing randomly oriented nanobelt like growth and from the scale mentioned in the SEM micrographs, thickness of one layer is found to be between 125 nm - 166 nm. The growth observed in these films can be attributed to the presence of dislocations or/and defaults. It is observed that with increasing concentrations of CdSe the compactness of these nano belts increases.

### 4.2 XRD studies

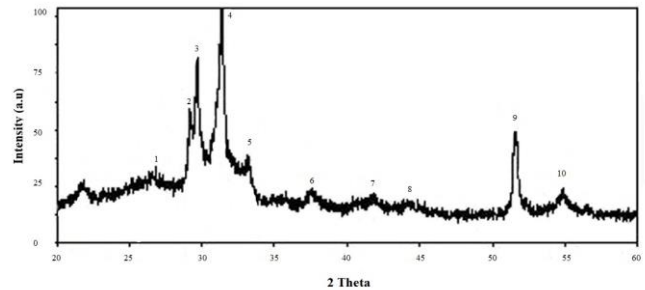


Fig. 2. X- ray diffractogram of CdS<sub>0.95</sub>Se<sub>0.05</sub> film.

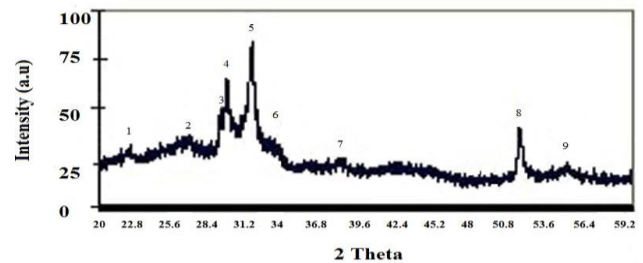


Fig. 3. X- ray diffractogram of CdS<sub>0.70</sub>Se<sub>0.30</sub> film.

Table 1. XRD data of  $CdS_{0.95}Se_{0.05}$  film.

S.No.	d-value (Å)		Relative Intensity (a. u.)		(h k l)	Lattice constant (Å)		Grain size/ dislocation density For (200) <sub>c</sub> CdS peak
	Observed	Reported	Observed	Reported		Observed	Reported	
1	3.35	3.36	30.27	100	(111) <sub>c</sub> CdS	a = 4.02	a = 4.13	13.04nm
2	3.05	3.1608	56.65	100	(101) <sub>h</sub> CdS	a = 3.99	a = 4.30	
3	3.01	3.28	78.83	65.7	(101) <sub>h</sub> CdSe	c = 6.923	c = 7.03	
4	2.84	2.90	100	40	(200) <sub>c</sub> CdS	a = 5.70	a = 5.82	
5	2.69	2.55	37	40	(102) <sub>h</sub> CdSe	c = 7.33	c = 7.03	
6	2.39	2.45	22.96	25	(102) <sub>h</sub> CdS	a = 4.06	a = 4.13	
7	2.15	2.15	20.98	82	(102) <sub>h</sub> CdS	a = 4.30	a = 4.30	
8	2.04	2.05	17.68	80	(110) <sub>h</sub> CdSe	a = 5.78	a = 5.82	
9	1.76	1.75	46.64	60	(220) <sub>c</sub> CdS	a = 5.85	a = 5.82	
10	1.67	1.68	23.08	10	(311) <sub>c</sub> CdS (222) <sub>c</sub> CdS	a = 5.79	a = 5.82	

Table 2. XRD data of  $CdS_{0.70}Se_{0.30}$  film.

S.No.	d-value (Å)		Relative Intensity (a. u.)		(h k l)	Lattice constant (Å)		Grain size/ dislocation density For (200) <sub>c</sub> CdS peak
	Observed	Reported	Observed	Reported		Observed	Reported	
1	3.86	3.72	21.76	23.90	(100) <sub>h</sub> CdSe	a = 4.45	a = 4.3	11.97nm
2	3.04	3.28	43.64	65	(101) <sub>h</sub> CdSe	a = 3.9	a = 4.3	
3	2.98	3.16	71.46	100	(101) <sub>h</sub> CdS	c = 6.54	c = 6.75	
4	2.81	2.90	91.84	40	(200) <sub>c</sub> CdS	a = 5.63	a = 5.82	
5	2.65	2.55	27.69	30	(102) <sub>h</sub> CdSe (400) <sub>c</sub> H <sub>2</sub> O <sub>3</sub>	a = 3.84	a = 3.84	
6	2.34	2.45	18.58	25	(102) <sub>h</sub> CdS	a = 3.86	a = 4.13	
7	2.11	2.15	17.38	82.49	(110) <sub>h</sub> CdSe	a = 4.29	a = 4.30	
8	1.76	1.75	43.16	60	(311) <sub>c</sub> CdS	a = 5.85	a = 5.82	
9	1.65	1.68	17.86	30	(222) <sub>c</sub> CdS	a = 5.82	a = 5.82	

Fig. 2 shows the X-ray diffractogram of  $\text{CdS}_{0.95}\text{Se}_{0.05}$  film. The corresponding data are presented in Table 1. The prominent peaks of cubic and hexagonal CdS and hexagonal CdSe are observed in this table showing a combination of independent lines of CdS and CdSe indicating formulation of a solid solution. The diffraction peaks are assigned using JCPDS data (CdS (cubic); JCPDS 10-454, CdS (hexagonal); JCPDS 41-1049 and CdSe (hexagonal) JCPDS 19- 191 by comparing the observed and reported values of the lattice constants. In this diffractogram, maximum intensity peak occurs at  $2\phi = 31.30^\circ$ , which can be assigned to cubic (200) CdS plane. Fig. 3 shows XRD of  $\text{CdS}_{0.70}\text{Se}_{0.30}$  film corresponding data is given in Table 2. If we compare Fig. 3 with Fig. 2, we observe a decrease in peak intensity and a slight broadening of FWHM ( $0.74^\circ$  from  $0.71^\circ$ ) which can be attributed to the decrease in particle size with increasing percentage of CdSe. The maximum intensity peak is similar in both the films. The particle size and dislocation densities are calculated for  $\text{CdS}_{0.95}\text{Se}_{0.05}$  and  $\text{CdS}_{0.70}\text{Se}_{0.30}$  films for (200) c peak of CdS [12]. The XRD studies show that the increasing selenium content i.e. anions, improves the hexagonal phase as indicated by the emergence of new hexagonal peaks of CdS/ CdSe. The average dislocation densities evaluated for these films from XRD studies are found to lie in the range  $4.93\text{-}9.58 \times 10^{15}$  lines/  $\text{m}^2$ .

### 4.3 Optical absorption spectral studies

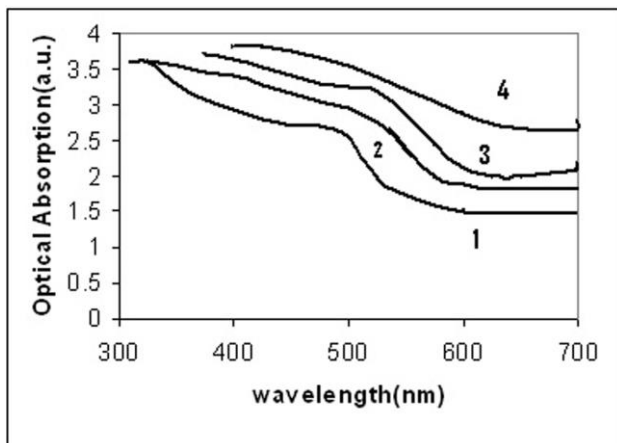


Fig. 4. Optical Absorption Spectra of various CdSSe films: 1 – CdS film 2 –  $\text{CdS}_{0.95}\text{Se}_{0.05}$  film, 2 –  $\text{CdS}_{0.90}\text{Se}_{0.10}$  film, 3 –  $\text{CdS}_{0.80}\text{Se}_{0.20}$  film, 4 –  $\text{CdS}_{0.70}\text{Se}_{0.30}$  film.

Fig. 4 shows the optical absorption spectra of different CdS-Se films. The optical absorption increases as the selenium content increases. As discussed in section 3.2 the thickness of the films increase with increasing percentage of selenium which in turn increases the optical absorption. Further, a constant absorption in the near IR region is observed in all the absorption curves, with a steep increase at the onset of direct photon transitions around 500nm.

The steepness parameter of the absorption curves of films is related to the additional disorder in the lattice leading to the deformation of the energy bands in the process of formation of solid solutions. The steepness of these curves is decreased as the percentage of CdSe increases.

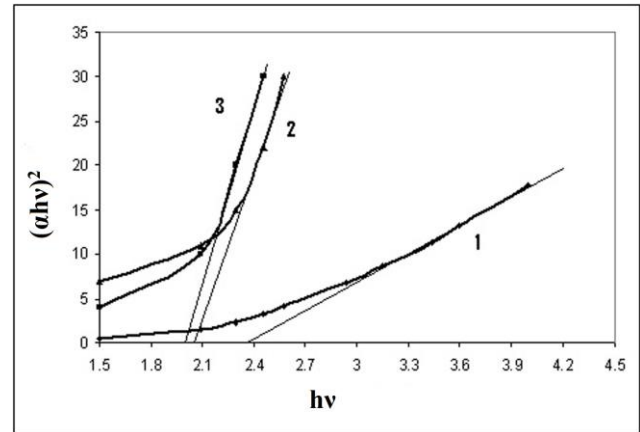


Fig. 5. Tauc's plot for various CdS-Se films: 1.  $E_g = 2.42\text{eV}$  for CdS, 2.  $E_g = 2.21\text{eV}$  for  $\text{CdS}_{0.70}\text{Se}_{0.30}$ , 3.  $E_g = 2.36\text{eV}$  for  $\text{CdS}_{0.95}\text{Se}_{0.05}$ .

The band gaps were calculated from the Tauc's plot of  $(\alpha h\nu)^2$  Vs  $(h\nu)$  for the optical absorption spectra of different CdS-Se films shown in Fig. 5. This plot shows the direct band gap nature of the films. A decrease in the band gap with increasing percentage of CdSe is also observed which suggests the formation of a common lattice through solid solution for different proportions of S/ Se in CdS-Se films as also observed in the XRD studies.

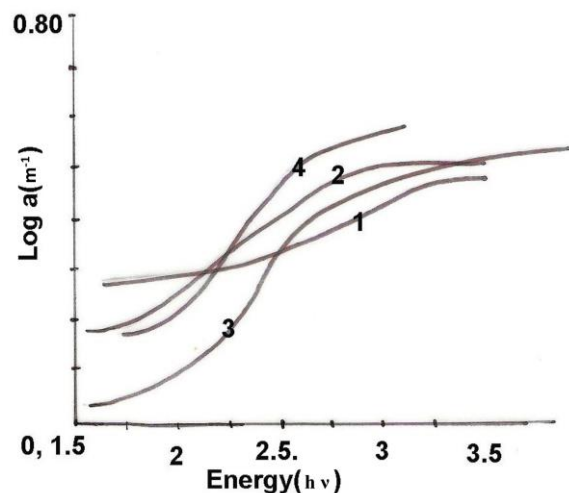


Fig. 6. (a) Variation of Urbach energy with temperature RT- 1.57eV 2.  $60^\circ\text{C}$ - 1.75 eV 3.  $70^\circ\text{C}$ - 1.9eV 4.  $80^\circ\text{C}$ - 2.15eV.

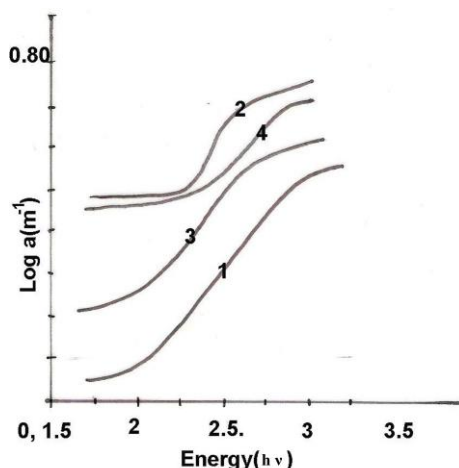


Fig. 6. (b): Variation in Urbach energy with composition. 1. CdS - 1.8 eV, 2. CdS<sub>0.95</sub>Se<sub>0.05</sub> - 1.9 eV, 3. CdS<sub>0.70</sub>Se<sub>0.30</sub> - 2.0 eV, 4. CdS<sub>0.60</sub>Se<sub>0.40</sub> - 2.0 eV.

The exponential spectral dependence of absorption is shown as low energy tails of many semiconductors referred to as Urbach energy [6]. This was calculated from the slope of the  $\log \alpha$  vs.  $h\nu$  graph shown in Fig. 6, for different films prepared with (a) different deposition temperature and also (b) at different concentrations of CdSe.

The steepness of the slopes of these graphs characterizes the width of exponential band-tailing into the gap and is frequently used as a measure of disorder and impurities in thin films [13].

As observed in Fig. 6(a) & (b) all the graphs for the spectral response of  $\log \alpha$  show a sharp increase in the vicinity of the band gap region (between 2 and 2.5 eV) and then a saturation is obtained. However the steepness of the graphs varies with composition or temperature of the chemical bath during preparation. The Urbach energy remains unchanged ( $\sim 2$  eV) with respect to the compositional changes i. e. with variation in the S/Se ratio, but increases with the increasing deposition temperature of the films. Similar results have been reported earlier by Siemson and Stuke [14, 15].

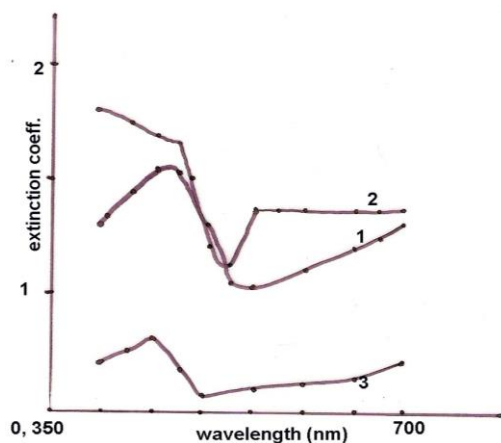


Fig. 7. Effect of selenium content Spectra on the extinction coefficient of: 1. CdS film, 2. CdS<sub>0.95</sub>Se<sub>0.05</sub> film 3. CdS<sub>0.70</sub>Se<sub>0.30</sub> film.

Fig. 7 shows the spectra of extinction coefficient 'k' in the visible region for three representative films of CdS-Se. As per the formula mentioned in section 3.2 k is proportional to the optical absorption coefficient. Comparing Fig. 4 with Fig. 7 we observe that the general behaviour of the curves are similar for both k and  $\alpha$  except for CdS<sub>0.70</sub>Se<sub>0.30</sub> films for which the magnitude of the extinction coefficient shows a remarkable decrease. As mentioned in section 3.2 the thickness of the films increased with increasing selenium content and 'k' is inversely proportional to the thickness of films. The difference in thicknesses of CdS and CdS<sub>0.95</sub>Se<sub>0.05</sub> films is less as compared to that between CdS and CdS<sub>0.70</sub>Se<sub>0.30</sub> prepared under similar conditions, so we observe a greater decrease in 'k' values in this case.

#### 4.4 Reflectance spectral studies

According to the formula shown in section 3 factor of  $n/ns$  reflects the fact that the energy carried by an EM wave is proportional to its phase velocity as given by the index of refraction. So the reflectance depends on the thicknesses as well as the refractive indices of the films and varies accordingly. In present study it was observed that the thickness and hence the absorption increases with increase in selenium content as discussed earlier. Hence reflectance goes down (i.e. transmittance increases) for films with higher selenium content.

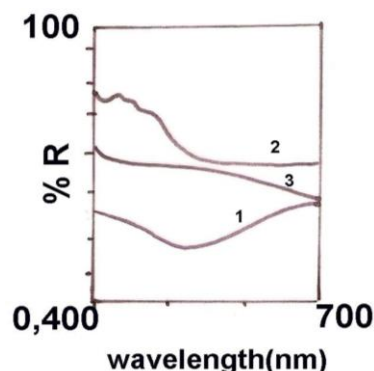


Fig. 8. Variation in reflectance with wavelength: 1. CdS, 2. CdS<sub>0.95</sub>Se<sub>0.05</sub>, 3. CdS<sub>0.70</sub>Se<sub>0.30</sub>.

Fig. 8 shows the reflectance spectra of different CdS-Se films. The reflectance increases steeply in CdS<sub>0.95</sub>Se<sub>0.05</sub> film around 500 nm. Giant oscillations were observed near UV region in all the films, which are not shown in the figure as they are superimposed with the reflectance of the glass substrate. Further, in this region the absorption is changing abruptly, violating the basic assumptions used to derive the formulae mentioned in section 3. The reflectance spectrum of CdS<sub>0.70</sub>Se<sub>0.30</sub> film is almost constant in the visible region where as CdS film shows slow oscillations. The oscillations observed in the

reflectance spectra result from very smooth and thin films. As discussed earlier, the thickness of the films increases with the selenium content so the oscillations are not present in the reflectance spectra of thicker films.

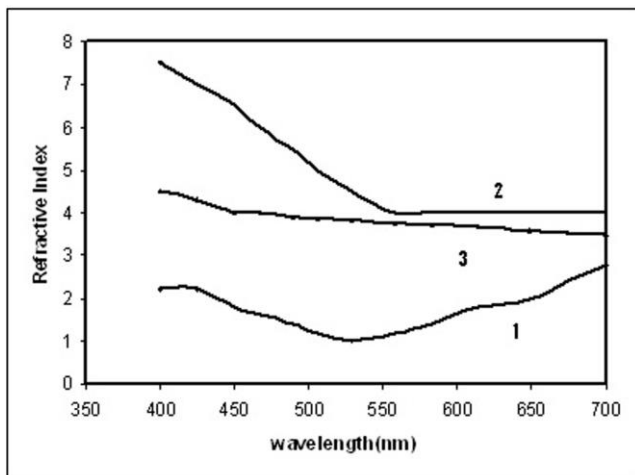


Fig. 9. Variation of refractive index with wavelength.  
1. CdS, 2. CdS<sub>0.95</sub>Se<sub>0.05</sub>, 3. CdS<sub>0.70</sub>Se<sub>0.30</sub>.

The refractive index can be calculated for normal incidence from the lower absorbance part of the films. Generally outside the region of fundamental absorption ( $h\nu > E_g$ ) or of the free-carrier absorption (for higher wavelengths), the dispersion of  $n$  and  $k$  is not very large [7]. If we assume that in a particular region, the film is weakly absorbing and the substrate is completely transparent, then using the formulae mentioned in section 3, the refractive index ( $n$ ) of the film on a transparent substrate can be evaluated from the transmission/reflectance spectra. In the visible spectral range (400nm to 700nm), these conditions are satisfied. We have calculated the values of refractive index and the variation with wavelength is shown in Fig. 9. Curve 1 shows a smooth linear variation throughout the visible range. The refractive index of CdS<sub>0.95</sub>Se<sub>0.05</sub> film (curve 2) is higher and shows abrupt increase in the region adjacent to the band gap, this can be related to the higher absorption in this region shown by this film. However that of CdS<sub>0.70</sub>Se<sub>0.30</sub> shows a decrease (curve 3) but remains almost constant throughout the visible spectra as in this case the absorption decreases and the thickness increases considerably as compared to other films. As mentioned in Table 1 and 2 the grain size of CdS<sub>0.95</sub>Se<sub>0.05</sub> film is greater than that of CdS<sub>0.70</sub>Se<sub>0.30</sub> film. Bigger grain size leads to the higher value of refractive index [16], which in turn increases the optical reflectance. Fig. 8 and Fig. 9 show a clear dependence of reflectance and refractive index on the grain sizes.

## 5. Conclusions

The present study shows a simple and cost effective method of preparation of CdS-Se nanobelt structures. The parameters like grain size and dislocation density were calculated from XRD studies. The band gap, Urbach energy and extinction coefficients were calculated through the absorption spectral studies. The variations in Urbach energy with temperature and composition of CdS-Se films were helpful in studying the defect structure of the materials. The reflectance spectral studies show the grain size dependence of refractive index of the material. This fact can be further exploited for the application of CdS-Se nano belts as waveguides.

## Acknowledgements

Author is grateful to UGC, Bhopal for providing funds, and also to IUC-DAE, Indore, for making facilities available for XRD and SEM studies.

## References

- [1] P. Srivastava, K. Singh, *Adv. Mat. Lett.* **3**(4), 340 (2012).
- [2] I-Shuo Liu, Hsi-Hsing Lo, Chih-Tao Chien, Yun-Yue Lin, Chun-Wei Chen, Yang-Fang Chen, Wei-Fang Su, Sz-Chian Liou, *J. Mater. Chem.* **18**, 675 (2008).
- [3] S. Saha, *J. Phys. Sci.*, **15**, 251 (2011).
- [4] K. L. Chopra, "Thin Film Phenomenon" Mc Graw Hill Inc., USA, 99-104 (1969).
- [5] S. Tolansky, "Multiple Beam Interferometry of Surfaces and Films," Oxford Univ. Press, Fair Lawn, N.J (1948).
- [6] F. Urbach, *Phys Rev.* **92**, 1324 (1953).
- [7] J. C. Manifacier, J. Gasiot, J. P. Fillard, *J. Phys. E*, **9**, 1002 (1976).
- [8] R. Swanepoel, *J Phys E*, **16**, 1214 (1983).
- [9] P. Scherrer, *Göttinger Nachrichten Gesell.* **2**, 98 (1918).
- [10] B. D. Cullity, *Elements of X-ray diffraction.* Reading, MA: Addison-Wesley. 514, (1967).
- [11] G. K. Williamson, R. E. Smallman, *Phil. Mag.* **11**, 34 (1956).
- [12] H. P Klug, L. E. Alexander, *Ind Ed, N.Y.*, Wiley-Intersciences. 495 (1974).
- [13] A Aqili, A. Maqsood, *Applied Optics*, **41**, 219 (2002).
- [14] K. J. Siemson, E. W. Fenton, *Phys. Rev.* **162**, 632 (1967).
- [15] J. Stuke, *J. Noncryst.* **4**, 1 (1970).
- [16] K. Senthil, D. Mangalraj, K. Narayandass Sa, Adachi Sadao, *Mat. Sci. Eng. B* **78**, 53 (2000).

\*Corresponding author: anjalioudhia@gmail.com